Paper:

Cutting Performance of Coated Cemented Carbide Tool in Driven Rotary Cutting of Hardened Steel

Hideharu Kato[*1,†], **Noriyuki Takase**[*2], **Kentaro Watanabe**[*3], **Tatsuya Shikimura**[*4], **and Kazuyuki Kubota**[*5]

[*1]Kanazawa Institute of Technology
3-1 Yatsukaho, Hakusan, Ishikawa 924-0838, Japan
[†]Corresponding author, E-mail: hkato@neptune.kanazawa-it.ac.jp
[*2]Yokowo Co., Ltd., Tomioka, Japan
[*3]Toshiba Machine Co., Ltd., Numazu, Japan
[*4]Takamatsu Machinery Co., Ltd., Hakusan, Japan
[*5]Mitsubishi Hitachi Tool Engineering, Ltd., Yasu, Japan
[Received June 10, 2018; accepted October 9, 2018]

Recently, cutting has replaced grinding in the finishing process for hardened steel. However, tool damage is a major problem in high-efficiency operations that use high-speed cutting and high-feed rate conditions rather than more conventional cutting conditions. Therefore, a new cutting technique that can realize high-efficiency cutting is desired. In our previous study, the processing efficiency was improved three to five times compared with conventional hardened steel cutting by driven rotary cutting. Furthermore, to attain high efficiency, the resistance of the tool material to wear and oxidation must be improved. In this study, the cutting performance of tools with an Al-rich coating, which improves oxidation resistance, is investigated for high cutting speed applications. In the present experiments, the flank wear of the Al-rich tool was less than 40 μm at a high cutting speed of 2.51 m/s, even for a cutting length of 10.0 km. Additionally, the Al-rich tool wear advanced progressively without flaking. In contrast, the conventional TiAlN-coated tools exhibited serious failure at cutting lengths of 3.0 km. It is thought that the difference in the oxidation resistance of the two tools influenced the cutting performance. Therefore, the tool with the Al-rich coating can operate with a high efficiency even at high cutting speeds.

Keywords: driven rotary tool, hardened steel, coated cemented carbide tool, high-efficiency machining, oxidation resistance

1. Introduction

Hardened steel, which is one of the most difficult materials to machine, has excellent endurance and abrasion resistance. This material is used in numerous automobile parts, such as cams and crank shafts, for which high friction and cyclic loading are expected [1]. Grinding processes have generally been used for the finish machining of hardened steel. However, the machining efficiency of grinding is low. The development of a TiAlN-coated tool [2] and a cubic boron nitride (cBN) sintered tool [3, 4] with excellent wear resistance has led to the replacement of grinding processes by cutting that can achieve high versatility and high efficiency [5–10]. The realization of higher cutting efficiencies requires the implementation of cutting conditions with high speeds and feed rates beyond those of the recommended conditions. However, under such conditions, the tool life becomes extremely short as a result of significant tool wear and the failure of the cutting edge. For this reason, a new processing technique that improves wear and fracture resistance is needed.

In contrast, driven rotary cutting has been realized by the development of a multi-task machine tool combining the functions of a computer numerical control (CNC) lathe and a machining center. High-efficiency machining has been studied using this method [11–14]. In a previous study, it was shown that the feed rate can be increased in the driven rotary cutting of hardened steel such that the machining efficiency is three to five times that of conventional turning. Furthermore, in driven rotary cutting, the cutting temperature is reduced by approximately 130 K and the thrust force is reduced relative to that of conventional machining [15]. However, even under conditions that enable high efficiency, the cutting speed is at the conventional level (1.67 m/s), and the use of driven rotary cutting dose not increase the cutting speed. In addition, even in the high-speed driven rotary cutting of hardened steel, an increase in tool wear and tool oxidation are expected owing to the increase in the cutting temperature. Therefore, it would be beneficial to use a coating tool that has sufficient wear and oxidation resistance under high-speed cutting conditions.

In this study, the influence of increased cutting speed on cutting performance was investigated in the drive rotary cutting of hardened steel using Al-rich TiAlN-coated

Table 1. Chemical composition of DC53.

Chemical composition mass [%]									
C	Si	Mn	P	Ni	Cr	Mo	Cu	V	Fe
0.97	1.16	0.37	0.023	0.12	8.18	1.97	0.12	0.21	Bal.

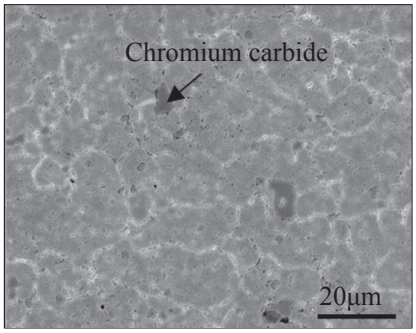

Fig. 1. SEM image of DC53 microstructure (etching solution: 3% Nital, time: 70 s).

tools under high-speed cutting conditions. Additionally, the mechanism of tool damage was investigated.

2. Experimental Procedures

2.1. Workpiece Material

In this study, a rotary cutting experiment was performed using cold-worked die steel (DC53) as the work material. The workpiece was a cylinder with a length of 500 mm and diameter of 60 mm. **Table 1** shows the chemical composition of DC53. **Fig. 1** shows a scanning electron microscopy (SEM) image of the microstructure of DC53, where chromium carbide can be seen in the martensitic structure. During quenching, a hardened layer with a hardness of approximately 770 HV is formed on DC53.

2.2. Rotary Tool Material and Geometry

The TiSiN-TiAlN coated tool described in **Table 2** was used in the experiment. The tool substrate material was cemented carbide (Z01) coated with an inner TiAlN film and an outer TiSiN film to a total thickness of approximately 2.0 μm. For the TiAlN film of tool A, the Ti : Al ratio was 1 : 1. In the case of tool B, the Ti : Al ratio was set to 1 : 1.3 to improve the resistance to oxidation [16–18]. A honing treatment was applied to the cutting edges of both tools. **Fig. 2** shows a SEM image of the cutting edge. Numerous droplets were observed on the tool surface after coating, as shown in **Fig. 2(a)**. To reduce the potential influence of these droplets, an aero lap treatment was performed, which resulted in the surface shown in **Fig. 2(b)**. The tool was a simple cylinder with dimensions of $\phi 10 \times 75$ mm.

Table 2. Cutting tools.

Tool	Substrate material	Film material		Ratio of Ti : Al in TiAlN films
		1st	2nd	
Tool A	Z01	TiAlN	TiSiN	1:1
Tool B				1:1.3

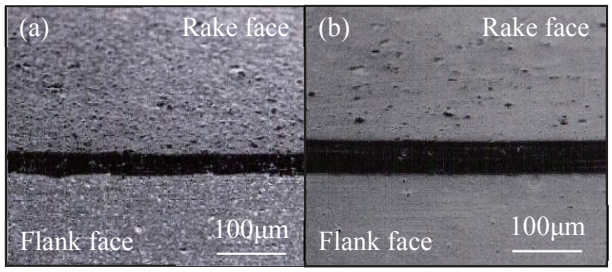

Fig. 2. Cutting edge of tool used in experiment; (a) before aero lap treatment, and (b) after aero lap treatment.

Table 3. Cutting conditions.

Velocity of workpiece V_w [m/s]	1.67	2.51	3.34
Velocity of tool V_t [m/s]	0.52	0.78	1.04
Speed ratio V_t/V_w [–]	0.31		
Feed rate f [mm/rev]	0.3		
Depth of cut d [mm]	0.1		
Cutting method	Tool spindle: forward Work spindle: reverse		
Cutting environment	Dry, Wet, DIPS		

2.3. Cutting Conditions

Table 3 shows the experimental conditions. The velocity, V_w, of the workpiece was set to 1.67, 2.51, and 3.34 m/s. The corresponding velocities, V_t, of the tool were 0.52, 0.78, and 1.04 m/s, respectively, such that a speed ratio, V_t/V_w, of 0.31 was maintained in all cases. The feed rate, f, was 0.3 mm/rev. The cutting method was a combination of forward rotation of the tool spindle and reverse rotation of the work spindle. Three cutting environment conditions, namely dry, wet, and injection of micro dry ice using compressed air (DIPS), were considered. A multitasking machine tool (XB1000: Takamatsu Machinery Co., Ltd.) was used to perform the driven rotary cutting. **Fig. 3** shows a schematic diagram of the rotary cutting setup. The workpiece material was fixed by chucking both sides of the workpiece. A tool was attached to the tool spindle, and rotated coercively with the tool spindle. The tool and workpiece spindles were rotated simultaneously and turning was performed. The cutting edge-position was shifted by 10° with respect to the Y-axis so that the rake angle of the tool was $-10°$ and the clearance angle was 10°. The tool run-out at the time of the experiment was 10 μm or less. The tool life was

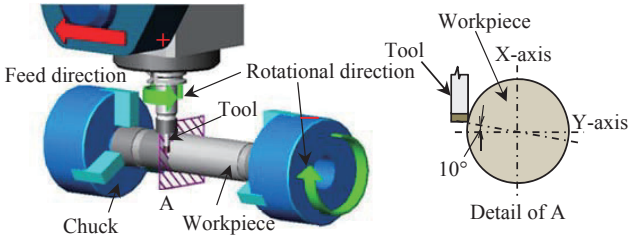

Fig. 3. Schematic illustration of experimental setup.

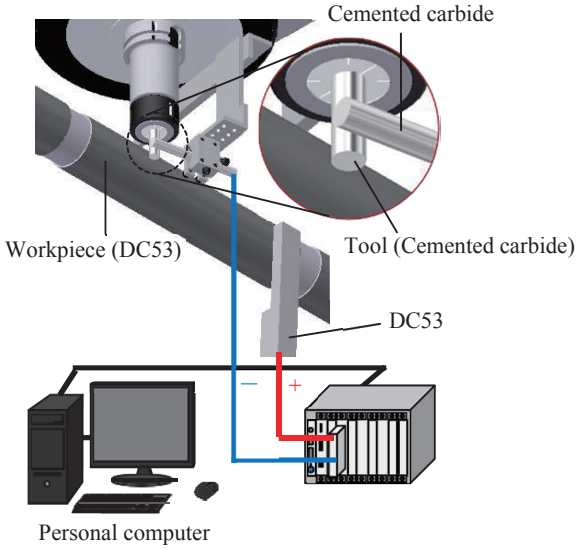

Fig. 4. Schematic illustration of thermal electromotive force measurement.

characterized as the time at which the flank wear width reached 100 μm or failed at the cutting edge circumference. This experiment was performed twice or three times under all conditions.

2.4. Measurement of Cutting Temperature

Figure 4 shows the tool-workpiece (T-W) method for the measurement of the thermal electromotive force [15]. The thermal electromotive force was measured using a thermocouple between the tool material and the workpiece material. Subsequently, the thermal electromotive force was converted into the cutting temperature using a calibration curve for a cemented carbide and DC53 thermocouple obtained through earlier measurements.

2.5. Scratch Test

Figure 5 shows a schematic illustration of the scratch test equipment [19]. The scratch tests were conducted under the conditions shown in **Table 4**. A vertical load was applied via a conical diamond indenter with a tip curvature radius of 25 μm, which moved at a speed of 0.2 mm/s. The scratch tests were performed at loads ranging from 7.0 to 8.5 N in increments of 0.5 N. The

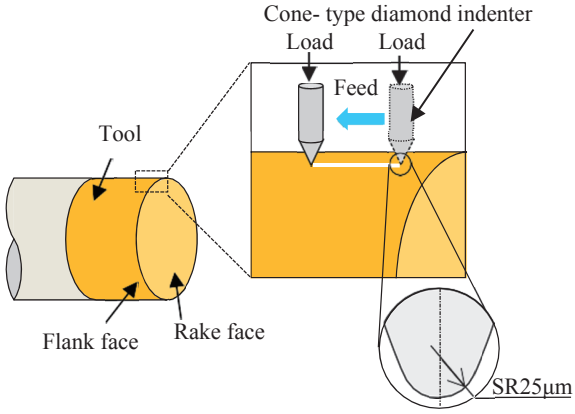

Fig. 5. Schematic illustration of scratch tests.

Table 4. Conditions for scratch test.

Load F [N]	7.0–8.5
Scratch speed V_s [mm/s]	0.2
Curvature radius of cone-type diamond indenter R_c [μm]	25
Temperature θ [K]	293

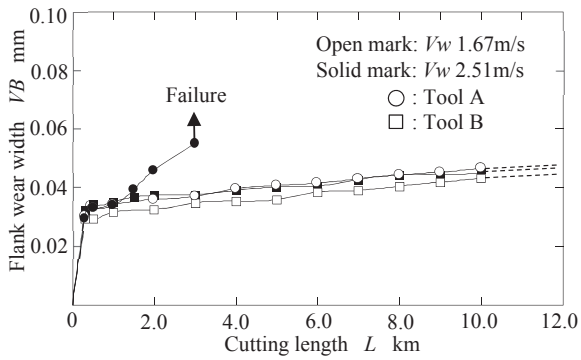

Fig. 6. Relationship between cutting length and flank wear width of tools A and B at each cutting speed.

critical load L_c was defined as the minimum load that produced a continuous scratch mark. Moreover, a film on the cylindrical surface of the tool was used in this test.

3. Experimental Results and Discussion

3.1. Influence of Tool Film Al Content and Cutting Speed on Tool Life

Figure 6 shows the relationship between the cutting length and the flank wear width for tools A and B at each cutting speed. The flank wear of tools A and B was less than 40 μm at a cutting speed of 1.67 m/s, even for a cutting length of 10.0 km. However, the cutting performance of tool B remained the same as the cutting speed was increased from 1.67 to 2.51 m/s, whereas the lifespan of tool A was reduced at a cutting speed of 2.51 m/s,

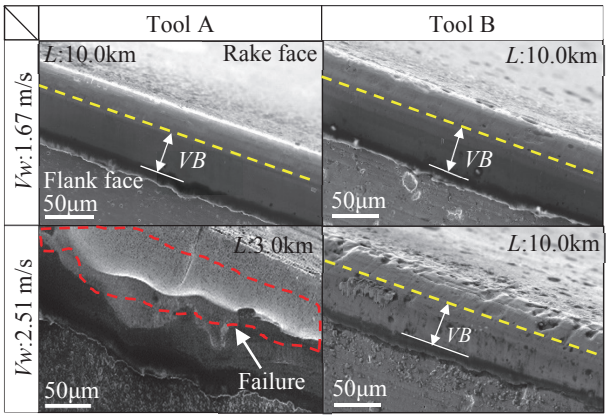

Fig. 7. Comparison of cutting edge for tools A and B at each cutting speed.

as it failed at a cutting length of 3.0 km. **Fig. 7** shows SEM images of the cutting edge of each tool for each cutting speed after a cutting length of 10.0 km, except in the case of tool A at 2.51 m/s, which is shown after failure at a cutting length of 3.0 km. At a cutting speed of 1.67 m/s and a cutting length of 5.0 km, the flank wear width for each tool was confirmed to be uniform without flaking. Furthermore, the wear condition of tool B at a cutting speed of 2.51 m/s was the same as that at a cutting speed of 1.67 m/s. In contrast, tool A at a cutting speed of 2.51 m/s was subject to serious failure after a cutting length of 3.0 km.

Figure 8 shows the progression of the cutting edge wear for tool A with increasing cutting length at a cutting speed of 2.51 m/s. Flaking of the film coating on the cutting edge was observed at a cutting length of only 0.1 km. The flaking increased with increasing cutting length and led to failure, and a crack was confirmed to have formed inside and surrounding the flaked area. Finally, the failure increased by crack propagation as the cutting length increased.

A detailed observation of the cutting edge was carried out to clarify the factors that rapidly expanded the chipping. Here, the cutting edge of the rotary tool is the outer periphery of the end face of the cylindrical tool, and damage to the cutting edge prior to chipping was also observed. Therefore, the cutting edge after acid treatment with aqua regia was observed. As shown in **Fig. 9**, the energy-dispersive X-ray spectrum obtained from the flaking point at a cutting length of 3.0 km was confirmed to exhibit peaks from the presence of W. However, it was confirmed that flaking was not observed on the same surface at a cutting length of 1.5 km. This indicates that the damage to tool A at a cutting speed of 2.51 m/s likely resulted in flaking. In contrast, **Fig. 10** shows the observation and analysis results of the cutting edge of tool B after 10.0 km of cutting at a cutting speed of 2.51 m/s. From this figure, the flaking on the rake face was not observed, and it is clear from the result of the component analysis that the coating remained. The coating film was only the first layer of Al-rich TiAlN, and this tendency

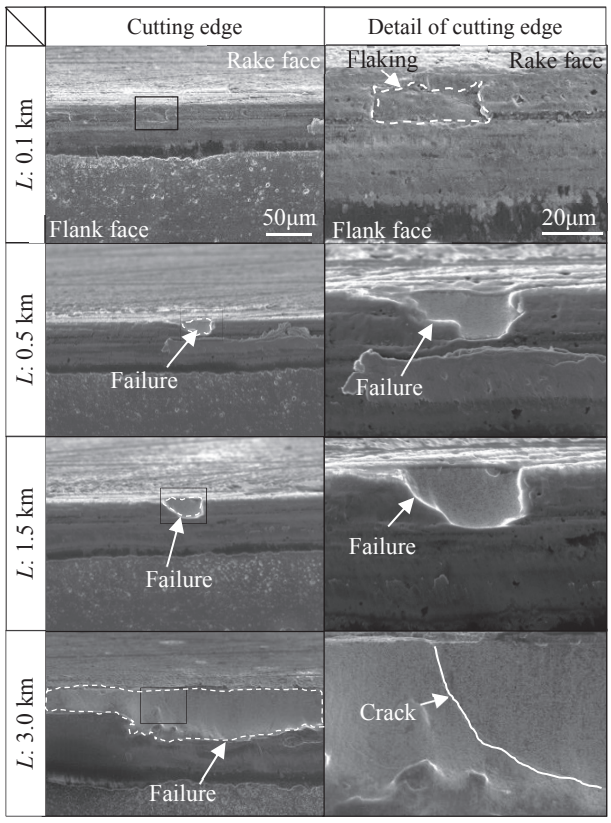

Fig. 8. Progress of cutting edge wear for tool A at different cutting lengths with cutting speed of 2.51 m/s.

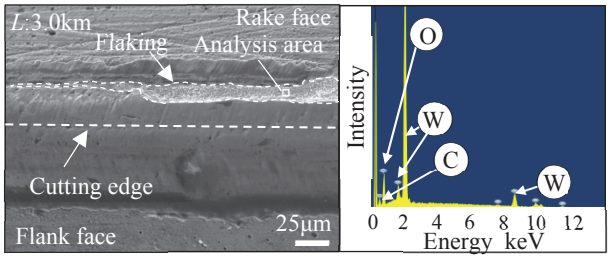

Fig. 9. SEM image and EDX analysis of tool A for cutting edge at cutting speed 2.51 m/s (*L*: 3.0 km).

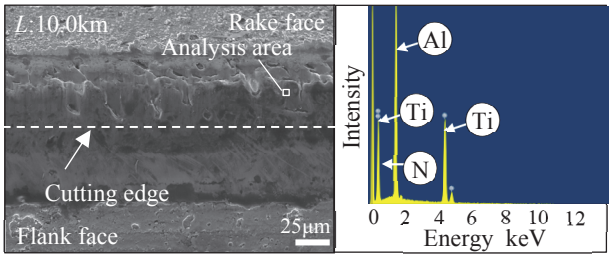

Fig. 10. SEM image and EDX analysis of tool B for cutting edge at cutting speed 2.51 m/s (*L*: 10.0 km).

is similar to that at the initial cutting length of 1.0 km. Although the area surrounding the cutting edge was observed, flaking was not confirmed. Therefore, in the case

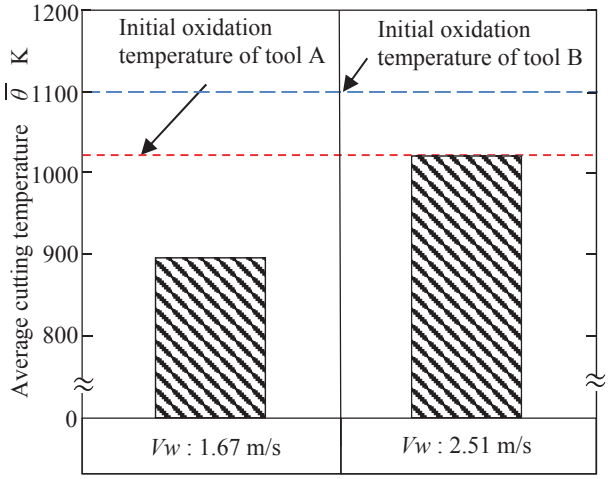

Fig. 11. Comparison of average cutting temperature at different cutting speeds.

of tool B, flaking of the coated film did not occur on the rake face; thus, it seems that a sufficient cutting edge was maintained at a cutting length of 10.0 km.

3.2. Investigation of the Effect of Damage of Coating Film on Difference in Cutting Speed

From the aforementioned results, the adhesive force of the film was evaluated and the cutting temperature was measured to investigate the mechanism of the coated-film damage. **Fig. 11** shows the comparison of cutting temperature at different cutting speeds. The dotted line in this figure is the initial oxidation temperature of both tools. The cutting temperature was approximately 890 K at the lower cutting speed of 1.67 m/s, but was substantially higher at 1023 K at the higher cutting speed of 2.51 m/s. In addition, the initial oxidation temperature of the TiAlN coating in tool A is approximately 1023 K [20]. This means that tool A is expected to oxidize at a cutting speed of 2.51 m/s. Therefore, tool A experiences flaking of the coating film and tool failure. In contrast, the initial oxidation temperature of the Al-rich TiAlN coating of tool B was approximately 1103 K [2], which is higher than the cutting temperature at a cutting speed of 2.51 m/s; this inhibits oxidation-induced flaking.

Therefore, the components of the coating on both tools were analyzed after cutting at a cutting speed of 2.51 m/s. **Fig. 12** shows the analysis results of the components of the coated film on the rake face of tool A. Since the peak of O was detected separately from Ti and Al, which are components of the coating film, it is obvious that the coating film has already been oxidized. In addition, since the peak of Si was not detected, the TiSiN coating film of the second layer is already considered to be worn. As a result of the analysis similarly at a cutting length of 1.5 km, Si, but not O, was detected thus, it is considered that the TiSiN coated film was worn from a cutting length of 1.5 to 3.0 km. From these facts, it is assumed that damage to tool A is as follows. Initially the TiSiN coating is worn

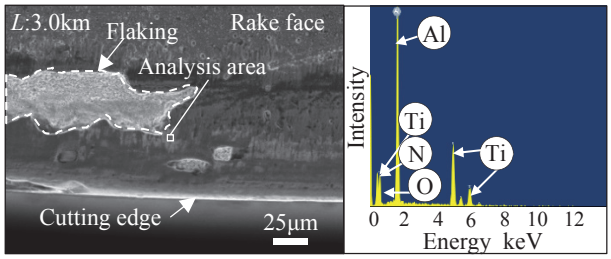

Fig. 12. SEM image and EDX analysis in tool A for rake face at cutting speed 2.51 m/s (L: 3.0 km).

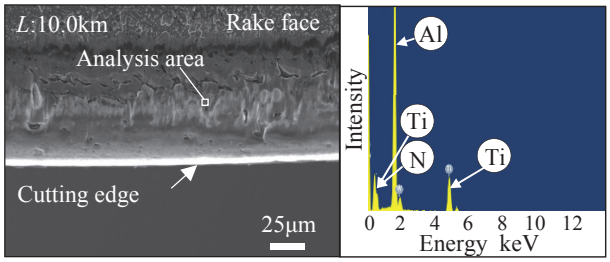

Fig. 13. SEM image and EDX analysis in tool B for rake face at cutting speed 2.51 m/s (L: 10.0 km).

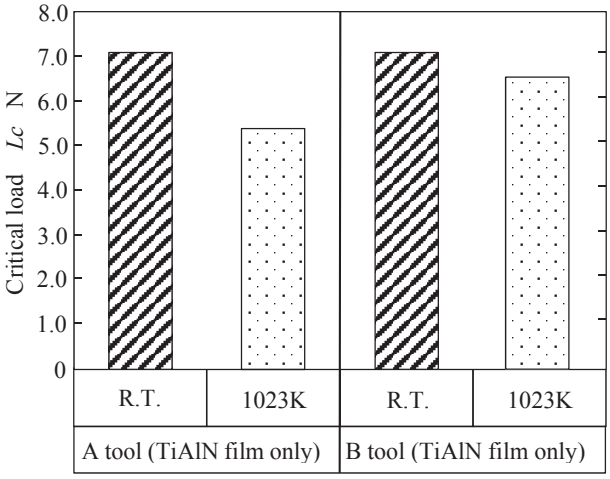

Fig. 14. Comparison of critical loads at room temperature (293 K) and after heat treatment for tools A and B.

and the TiAlN coating is exposed. Subsequently, oxidation of the TiAlN coating occurs, resulting in flaking.

In contrast, **Fig. 13** shows the analysis results of tool B, which reached the cutting length of 10.0 km at a cutting speed of 2.51 m/s. From the analysis results of tool B, the components of the coating film, such as Ti and Al, were detected; however, the peak of O was not detected. Furthermore, Si was not detected as with tool A. For this reason, it is considered that tool B suffered very little damage due to oxidation of the TiAlN film, and flaking of the coated film did not occur.

Here, the adhesion strength of the TiAlN film of both tools was measured. **Fig. 14** shows a comparison of the critical load for each tool. In each case, a scratch test was

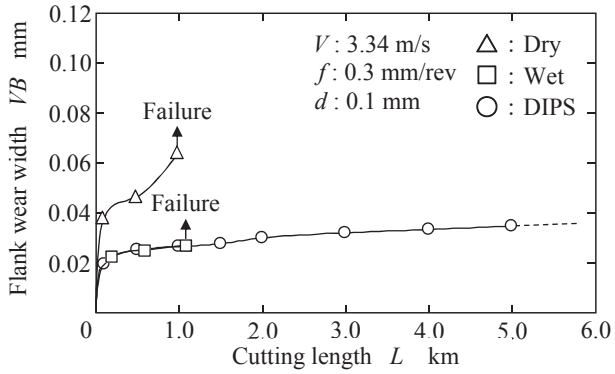

Fig. 15. Relationship between cutting length and flank wear width of tool A in each cutting environment at cutting speed 3.34 m/s.

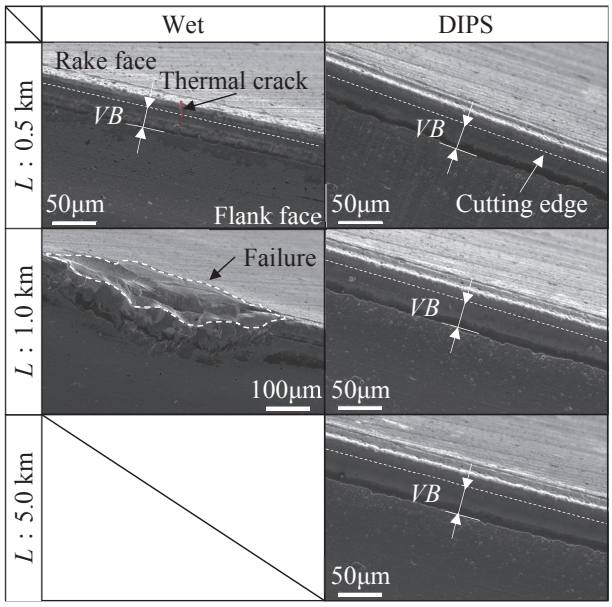

Fig. 16. Comparison of cutting edge of tool A with progress of cutting edge under wet and DIPS conditions.

conducted at room temperature (297 K) after heat treatment. Heat treatment was carried out by an electric furnace, heating up to 1023 K which is the same temperature as the cutting speed of 2.51 m/s, holding for 30 min, and air cooling. From this figure, the critical load at room temperature was 7.0 N for both tools and did not change. Conversely, differences were observed in both tools after heat treatment. The adhesion strength of tool A after the heat treatment showed a decrease of 1.5 N. In contrast, the adhesion strength of tool B after the heat treatment has a decrease of only 0.5 N. Therefore, it can be considered that the cutting temperature of tool A was almost equal to the oxidation starting temperature of the TiAlN coating at a cutting speed of 2.51 m/s, the TiAlN coating on the rake face was oxidized, and flaking of the coated film occurred. Moreover, the Al-rich TiAlN film of tool B did not oxidize, and tool defects did not occur despite the cutting length reaching 10.0 km. Thus, tool B can be used for high-efficiency cutting at a cutting speed of 2.51 m/s.

3.3. Effect of Different Cutting Environments on Tool Damage

To verify the cause of tool damage based on the results presented in the previous section, the influence of the cutting environment on the tool damage was investigated. High-efficiency is also discussed further.

Tool A was used in this investigation. The cutting conditions were as follows: the work material rotation speed, V_w, was 3.34 m/s, the tool rotation speed, V_t, was 1.04 m/s, the feed rate, f, was 0.3 mm/rev, and the depth of cut d was 0.1 mm. The cutting method was the same as in the previous section, and three cutting environments were considered: dry method (dry), wet method using a water-soluble oil agent (wet), and a micro dry ice powder supply method (DIPS).

Figure 15 shows the relationship between the cutting length and the flank wear width under each cutting condition. Under the dry condition, a remarkable increase in the wear width was observed from the initial cutting length, and the tool life was determined by failure at a cutting length of 1.0 km. Although the progression of the wear width was suppressed under the wet condition, the tool life was not extended, as failure still occurred at a cutting length of 1.0 km. In contrast to these conditions, the DIPS condition produced a wear width as small as 40 μm even when the cutting length reached 5.0 km, and the progression of the wear width was suppressed as in the wet condition. **Fig. 16** shows the progression of the damage of the tool cutting edge under the wet and DIPS conditions with increasing cutting length. As shown in this figure, the cutting edge of the tool under the DIPS condition exhibited no serious damage at any cutting length and gradually wore down. In contrast, under the wet condition, a crack perpendicular to the cutting edge formed at a cutting length of 0.5 km, and the tool life was determined at a cutting length of 1.0 km as a result of tool failure. Because the rotary tool uses the outer peripheral portion of the cylindrical end surface as a cutting edge, one point on the cutting edge was considered to be in the same state as the cutting edge in intermittent cutting. It was inferred that thermal cracks formed as a result of the severe temperature gradient between the heating caused by the cutting and the cooling caused by the cutting fluid [12].

Next, the damage factors in the dry and DIPS conditions were examined. **Fig. 17** shows the results of the component analysis of the tool rake face under these two cutting conditions. In the dry condition, Ti and Al, which are coating components, were detected in the vicinity of the film flaking, and an O was also detected. In contrast, under the DIPS condition, only the coating components, such as Ti and Al, were detected, and no O peak was observed. These results indicate that the coating oxidizes under dry conditions.

The cutting temperature was measured under the three cutting conditions, and the results are shown in **Fig. 18**. As shown in the figure, the average cutting temperature

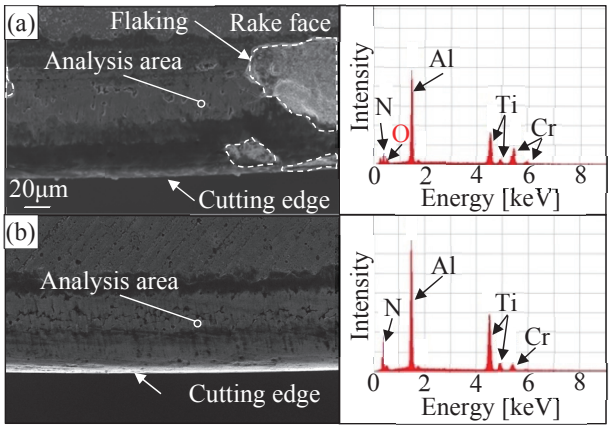

Fig. 17. Comparison of SEM image and EDX analysis under both conditions; (a) dry, $L = 1.0$ km and (b) DIPS, $L = 5.0$ km.

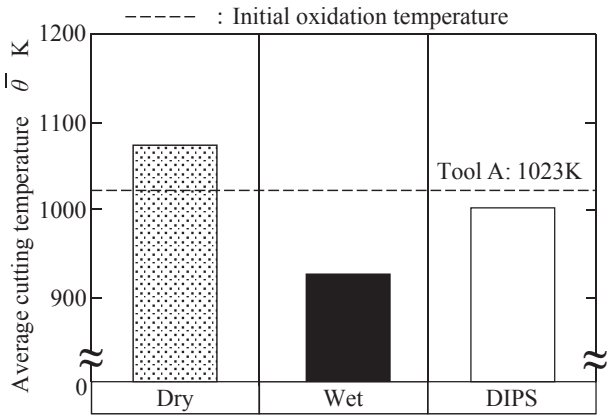

Fig. 18. Comparison of average cutting temperature for each cutting environment.

of the dry condition was approximately 1077 K. This means that the coating was oxidized, because the oxidation onset temperature of the TiAlN coating is approximately 1023 K [20] and the average cutting temperature of the dry condition exceeded this temperature. The flaking of the coating film was considered to be caused by the oxidation of the coating film. In contrast, the average cutting temperature of the DIPS condition was approximately 1006 K. The average cutting temperature of the DIPS condition was 17 K lower than the oxidation onset temperature of the coating. However, the actual cutting temperature tends to be higher than the average temperature, and it is presumed that the DIPS condition was also affected by oxidation like the dry condition; however, the coating film damage did not occur. Therefore, the carbon dioxide sublimed when micro dry ice was supplied remains in the vicinity of the cutting point. Thus, it is considered that the oxygen concentration was also lowered to suppress the oxidation of the coating film.

From these results, it is concluded that both the improvement in the oxidation resistance of the tool coating and the preparation of a cutting environment in which oxidation is difficult can enable high-efficiency processing by allowing operation at high cutting speeds.

4. Conclusion

In the present study, the cutting performance of an Al-rich coated tool with improved oxidation resistance was investigated under high cutting speed conditions. The obtained results are summarized as follows.

(1) The flank wear width was less than 40 μm for tools A and B at a cutting speed of 1.67 m/s, even when the cutting length exceeded 10.0 km.

(2) The failure of tool A occurred at a workpiece cutting speed of 2.51 m/s and a cutting length of 3.0 km, and the exposure of the cemented carbide tool substrate was confirmed at the cutting edge. In contrast, the flaking of the film coating on tool B was suppressed by its improved oxidation resistance.

(3) Tool B can be used for high-efficiency cutting at a cutting speed of 2.51 m/s.

(4) The flaking of the coated film was confirmed near the cutting edge, and a cutting speed of 2.51 m/s for tool A resulted in serious failure at a cutting length of 3.0 km.

(5) The adhesion strength of tool B after the heat treatment exhibited a decrease of only 0.5 N, and the decrease in adhesion strength is small compared with that of tool A.

(6) The cutting temperature at a cutting speed of 2.51 m/s was 1023 K, which is the initial oxidation temperature of the TiAlN coating of tool A.

(7) Although the progression of the wear width was moderate under the wet condition at a cutting speed of 3.34 m/s, thermal cracks formed during the initial cutting stage, causing failure at a cutting length of 1.0 km.

(8) In the DIPS condition, the progression of the wear was moderate and gradual. Damage to the coated film was suppressed even at a cutting speed of 3.34 m/s, enabling high-efficiency cutting. Moreover, it is considered that the oxygen concentration was also lowered as a factor with which to suppress the oxidation of the coating film.

References:

[1] Y. Okada, "Trends of Structural Steels for Automobiles," Denki Seiko (Electr. Furn. Steel), Vol.69, No.1, pp. 49-56, 1998.

[2] T. Ikeda and H. Satoh, "Phase formation and characterization of hard coatings in the Ti-Al-N system prepared by the cathodic arc ion plating method," Thin Solid Film, Vol.195, Issues 1-2, pp. 99-110, 1991.

[3] K. Shintani, M. Ueki, and Y. Fjimura, "Optimum Tool geometry of CBN tool for continuous turning of carburized steel," Int. J. of Machine Tools & Manufacture, Vol.29, Issue 3, pp. 403-413, 1989.

[4] K. Shintani, M. Ueki, and Y. Fjimura, "Optimum Cutting Tool geometry when interrupted cutting carburized steel by CBN tool," Int. J. of Machine Tools & Manufacture, Vol.29, Issue 3, pp. 415-423, 1989.

[5] T. Egawa, T. Ichikizaki, M. Kuroda, Y. Hiasa, and H. Tsukamoto, "Wear mechanism of cBN tool in cutting of hardened steel," The Japan Society for Precision Engineering, Vol.61, No.6, pp. 809-819, 1995.

[6] N. Narutaki, Y. Yamane, and M. Takeuchi, "Wear of CBN cutting tool," The Japan Society for Precision Engineering, Vol.45, No.2, pp. 201-207, 1979.

[7] Y. Yamada, T. Aoki, Y. Tanaka, and K. Wakihara, "Cutting Performance of Coated Carbide Tools for Hard Work Material," Trans. of the Japan Society of Mechanical Engineers, Vol.60, No.577, pp. 2906-2910, 1994.

[8] S. Enomoto and M. Kato, "Cutting characteristics of CBN cutting tools in turning chromium molybdenum steels of various hardnesses," The Japan Society for Precision Engineering, Vol.55, No.6, pp. 1079-1084, 1989.

[9] T.Ishikawa, F. Obata, and K. Inoue, "Wear mechanism of TiSiN-coated cutting tools on hgih-apeed cutting of hardened die steel," Japan Society for Precision Engineering, Vol.75, No.12, pp. 1439-1443, 2009.

[10] W. Konig, R. Fritsch, and D. Karnmermeier, "New approaches to characterizing the performance of coated cutting tools," CIRP Annals – Manufacturing Technology, Vol.41, Issue 1, pp. 49-54, 1992.

[11] S. Lei and W. Liu, "High-speed machining of titanium alloys using the driven rotary tool," Int. J. of Tools and Manufacture, Vol.42, Issue 6, pp. 653-661, 2002.

[12] H. Sasahara, A. Kato, H. Nakajima, H. Yamamoto, T. Muraki, and M. Tsutsumi, "High-speed rotary cutting of difficult-to-cut materials on multitasking lathe," Int. J. of Machine Tools and Manufacture, Vol.48, Issues 7-8, pp. 841-850, 2008.

[13] A. Hosokawa, T. Ueda, R. Onishi, R. Tanaka, and T. Furumoto, "Turning of difficult-to-machine materials with actively driven rotary tool," CIRP Annals – Manufacturing Technology, Vol.59, Issue 1, pp. 89-92, 2010.

[14] H. Sasahara, K. Satake, W. Takahashi et al., "The effect of oil mist supply on cutting point temperature and tool wear in driven rotary cutting," Precision Engineering, Vol.48, pp. 158-163, 2017.

[15] H. Kato, T. Shikimura, Y. Morimoto, K. Shintani, K. Kubota, and K. Nakagaki, "Study on High-efficiency finish turning of carburized hrdened steel with driven rotary cutting," Int. J. Automation Technol., Vol.7, No.3, pp. 321-328, 2013.

[16] T. Ikeda and H. Satoh, "High-temperature oxidation and wear resistance of Ti-Al-N hard coatings formed by PVD method," J. of the Japan Institute of Metals, Vol.57, No.8, pp. 919-925, 1993.

[17] A. Hörling, L. Hultman, M. Odén, J. Sjölén, and L. Karlsson, "Mechanical properties and machining performance of Ti1-xAlxN-coated cutting tools," Surface and Coatings Technology, Vol.191, Issues 2-3, pp. 384-392, 2005.

[18] A. Hörling, L. Hultman, and M. Odén, "Thermal stability of arc evaporated high aluminum-content Ti1-xAlxN thin films," J. of Vacuum Science & Technology, A 20, pp. 1815-1823, 2002.

[19] H. Kato, K. Ito, A. Kitamura, N. Ikenaga, and K. Kubota, "Study on milling of super elasto-plastic β type titanium alloy (Verification of processing characteristics and selection of optimum cutting conditions)," Trans. of the JSME, Vol.83, No.855, p. 17-00258, 2017.

[20] K. Yamamoto, T. Sato, K. Takahara, and K. Hanaguri, "Properties of (Ti,Cr,Al)N coatings with high Al content deposited by new plasma enhanced arc-cathode," Surface and Coatings Technology, Vols.174-175, pp. 620-626, 2003.

Name:
Hideharu Kato

Affiliation:
Professor, Kanazawa Institute of Technology

Address:
3-1 Yatsukaho, Hakusan, Ishikawa 924-0838, Japan

Brief Biographical History:
1993- Sumitomo Electric Industries, Ltd.
1995- Assistant Professor, Kanazawa Institute of Technology
2001- Associate Professor, Kanazawa Institute of Technology
2009- Professor, Kanazawa Institute of Technology

Main Works:
• "Study on milling of super elasto-plastic β type titanium alloy (Verification of processing characteristics and selection of optimum cutting conditions)," Trans. of the JSME, Vol.83, No.855, p. 17-00258, 2017.
• "Study on High-Efficiency Finish Turning of Carburized Hardened Steel with Driven Rotary Cutting," Int. J. Automation Technol., Vol.7, No.3, pp. 321-328, 2013.
• "A Study on the High-Efficiency Cutting of Austenitic Stainless Steel Using an HfN-Type Coated Tool," J. Advanced Mechanical Design, Systems, and Manufacturing, Vol.6, No.6, pp. 829-840, 2012.

Membership in Academic Societies:
• Japan Society for Precision Engineering (JSPE)
• Japan Society of Mechanical Engineers (JSME)
• Japan Society for Abrasive Technology (JSAT)

Name:
Noriyuki Takase

Affiliation:
Yokowo Co., Ltd.

Address:
1112 Kanohara, Tomioka-shi, Gunma 370-2495, Japan

Brief Biographical History:
2015- Graduate School, Kanazawa Institute of Technology
2017- Yokowo Co., Ltd.

Membership in Academic Societies:
• Japan Society of Mechanical Engineers (JSME)

Name:
Kentaro Watanabe

Affiliation:
Toshiba Machine Co., Ltd.

Address:
2068-3 Ohoka, Numazu-shi, Shizuoka 410-8510, Japan

Brief Biographical History:
2016- Graduate School, Kanazawa Institute of Technology
2018- Toshiba Machine Co., Ltd.

Membership in Academic Societies:
- Japan Society for Precision Engineering (JSPE)
- Japan Society of Mechanical Engineers (JSME)
- Japan Society for Abrasive Technology (JSAT)

Name:
Tatsuya Shikimura

Affiliation:
Takamatsu Machinery Co., Ltd.

Address:
1-8 Asahigaoka, Hakusan, Ishikawa 924-8558, Japan

Brief Biographical History:
2012- Graduate School, Kanazawa Institute of Technology
2013- Takamatsu Machinery Co., Ltd.

Main Works:
- "Study on High-Efficiency Finish Turning of Carburized Hardened Steel with Driven Rotary Cutting," Int. J. Automation Technol., Vol.7, No.3, pp. 321-328, 2013.

Membership in Academic Societies:
- Japan Society for Precision Engineering (JSPE)
- Japan Society of Mechanical Engineers (JSME)

Name:
Kazuyuki Kubota

Affiliation:
Plant Manager, Head of Coating Technology

Address:
35-2 Mikami, Yasu-shi, Shiga 520-2323, Japan

Brief Biographical History:
1990- Shibaura Institute of Technology
1994- Hitachi Tool Engineering, Ltd.
2015- Company name changed to Mitsubishi Hitachi Tool Engineering, Ltd.

Main Works:
- Hard coating on cutting tools

Membership in Academic Societies:
- Japanese Society for Tribologists (JAST)
- Surface Finishing Society of Japan (SFJ)